

Non-planar two-loop QCD corrections to $q\bar{q} \rightarrow \gamma\gamma\gamma$: finite remainders in the spinor-helicity formalism

Giuseppe De Laurentis

Albert-Ludwigs-Universität Freiburg

giuseppe.de.laurentis@physik.uni-freiburg.de

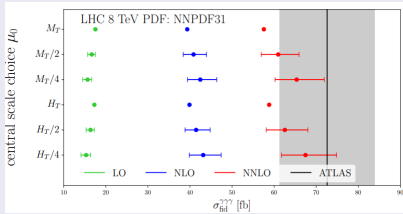
In collaboration with: S. Abreu, M. Klinkert, B. Page, and V. Sotnikov

arXiv:22xx:xxxxx

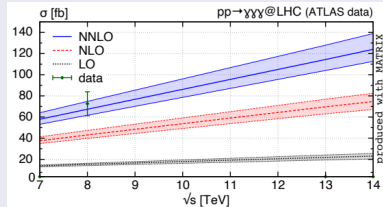
High Precision for Hard Processes
20th–22nd September 2022

Sizeable NNLO Corrections

Phenomenological studies with leading-color double-virtual amplitudes



Chawdhry, Czakon, Mitov, Poncelet (2019)



Kallweit, Sotnikov, Wiesemann (2020)

Analytic amplitudes in limit $N_c \rightarrow \infty$, $N_c/N_f = \text{const.}$

Chawdhry, Czakon, Mitov, Poncelet (2019, 2020); Abreu, Page, Pascual, Sotnikov (2020)

- Are subleading-color corrections truly negligible?

Gauge-Invariant Contributions at Two Loops

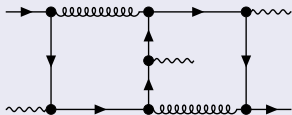
Four color-ordered amplitudes

- We can write the amplitude in terms of the $SU(3)$ Casimirs:

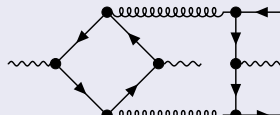
$$\mathcal{A}_{q\bar{q}\rightarrow\gamma\gamma\gamma}^{(2)} = C_F^2 B^{(2,0)} + C_F C_A B^{(2,1)} + C_F T_R N_f A^{(2,N_f)} + C_F T_R \left(\sum_{f=1}^{N_f} \frac{Q_f^2}{Q_{\text{ext.}}^2} \right) \tilde{A}^{(2,N_f)}$$

- Define: $A^{(2,0)} \equiv B^{(2,0)} + T_R^{-1} B^{(2,1)}$ and $A^{(2,1)} \equiv B^{(2,0)}$

- A Double-Pentagon for $A^{(2,1)}$



- A Hexagon-Box for $\tilde{A}^{(2,N_f)}$



- Only other 5-pt. process known w/ non-planar diags: $pp \rightarrow \gamma\gamma j$ [Ryan's talk]

Gauge-Invariant Contributions at Two Loops

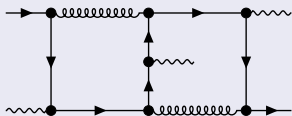
Four color-ordered amplitudes

- We can write the amplitude in terms of the $SU(3)$ Casimirs:

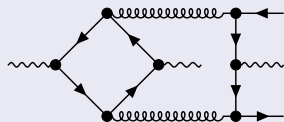
$$\mathcal{A}_{q\bar{q}\rightarrow\gamma\gamma\gamma}^{(2)} = C_F^2 B^{(2,0)} + C_F C_A B^{(2,1)} + C_F T_R N_f \underbrace{A^{(2,N_f)}}_{\text{Leading color, planar, already known}} + C_F T_R \left(\sum_{f=1}^{N_f} \frac{Q_f^2}{Q_{\text{ext.}}^2} \right) \tilde{A}^{(2,N_f)}$$

- Define: $\underbrace{A^{(2,0)}}_{\text{Leading color, planar, already known}} \equiv B^{(2,0)} + T_R^{-1} B^{(2,1)}$ and $A^{(2,1)} \equiv B^{(2,0)}$

- A Double-Pentagon for $A^{(2,1)}$



- A Hexagon-Box for $\tilde{A}^{(2,N_f)}$



- Only other 5-pt. process known w/ non-planar diags: $pp \rightarrow \gamma\gamma j$ [Ryan's talk]

Gauge-Invariant Contributions at Two Loops

Four color-ordered amplitudes

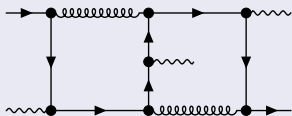
- We can write the amplitude in terms of the $SU(3)$ Casimirs:

$$\mathcal{A}_{q\bar{q}\rightarrow\gamma\gamma\gamma}^{(2)} = C_F^2 B^{(2,0)} + C_F C_A B^{(2,1)} + C_F T_R N_f A^{(2,N_f)} + C_F T_R \left(\sum_{f=1}^{N_f} \frac{Q_f^2}{Q_{\text{ext.}}^2} \right) \tilde{A}^{(2,N_f)}$$

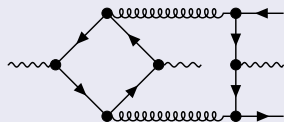
Subleading color, non-planar, new

- Define: $A^{(2,0)} \equiv B^{(2,0)} + T_R^{-1} B^{(2,1)}$ and $\tilde{A}^{(2,1)} \equiv B^{(2,0)}$

- A Double-Pentagon for $A^{(2,1)}$



- A Hexagon-Box for $\tilde{A}^{(2,N_f)}$



- Only other 5-pt. process known w/ non-planar diags: $pp \rightarrow \gamma\gamma j$ [Ryan's talk]

Numerical Generalized Unitarity with Caravel



Unitarity cuts

- Master-surface integrand decomposition Ita (2015)
- Unitarity-compatible IBPs via syzygies Gluza, Kajda, Kosower (2011)
- Two-loop D -dimensional unitarity cuts in Caravel
Abreu, Dormans, Febres Cordero, Ita, Kraus, Page, Pascual, Ruf, Sotnikov (2020)

$$\sum_{\text{states}} \prod_{i \in \text{Trees}_{\Gamma}} \mathcal{A}_i^{(0)}(\ell_l^{\Gamma}) = \sum_{\substack{\Gamma' \geq \Gamma \in \text{Topos.} \\ i \in \text{Master}_{\Gamma'} \cup \text{Surface}_{\Gamma'}}} \frac{c_{\Gamma',i} m_{\Gamma',i}(\ell_l^{\Gamma})}{\prod_{j \in (P_{\Gamma'} \setminus P_{\Gamma})} \rho_j(\ell_l^{\Gamma})}$$

Improvements for this calculation

- New surface terms for non-planar topologies;
- Retention of little group info throughout the computation.
 \Rightarrow Needed for spinor-helicity reconstruction.

The Focus of this Talk

Finite remainders (not normalized by the tree)

- Renormalize the amplitude and subtract universal IR poles:

$$\mathcal{R}_{\text{helicity}}^{(2\text{-loop})} = \sum_i r_i(\lambda, \tilde{\lambda}) h_i(\lambda, \tilde{\lambda})$$

- h_i : Pentagon functions [Chicherin, Sotnikov \(2020\)](#); r_i : **Rational functions**.

Spinor-helicity reconstruction and more

- Reconstruction of the r_i in spinor variables, [DL, Maître \(2019\)](#); [DL, Page \(2022\)](#)
for the first time with finite fields only [von Manteuffel, Schabinger \(2014\)](#); [Peraro \(2016\)](#)
- Simplification of bases of vector spaces of rational functions (new?)
- Exploitation of the symmetries of the amplitude (new at 2-loop?)

Why spinors? They better reflect the singularities in \mathbb{C}^{4n} , thus

- Need less numerical samples; \bullet More compact, stable and fast results.

Rational Coefficients & Common Denominators

Rational pentagon-function coefficients on common denominator

$$r_i(\lambda, \tilde{\lambda}) = \mathcal{N}_i(\lambda, \tilde{\lambda}) / \prod_j \mathcal{D}_j(\lambda, \tilde{\lambda})^{q_{ij}}$$

Singularities of the remainders

- Massless five-point finite remainders r_i have up to 35 poles

$$\mathcal{D}_j \in \{ \langle 12 \rangle, \langle 1|2+3|1 \rangle \} + \text{Permutations}(\{1, 2, 3, 4, 5\}) \& \lambda \leftrightarrow \tilde{\lambda}.$$

Degrees via (anti-)holomorphic shifts

see B. Page's SAGEX lectures (2021)

- The least common denominators can be obtained via

$$\overset{(\sim)}{\lambda}_i \rightarrow \overset{(\sim)}{\lambda}_i + t c_i \overset{(\sim)}{\eta} + \text{univariate reconstruction in } t$$

The Space of Pentagon Function Coefficients

Vector Spaces of Rational Functions

$$\mathcal{R}_{\text{hel.}}^{(l)} = r_i h_i = \tilde{r}_j M_{ji} h_i \text{ with } M_{ji} \in \mathbb{Q} \text{ and } \tilde{r}_j \text{ a basis of } \text{span}(r_i)$$

Common Denominator Basis Data

Contribution	$\#r_i$	$\dim(\text{span}(r_i))$	Largest mass dim. & assoc. phase weights	Common Den. Ansatz Size
$\tilde{\mathcal{R}}_{+++}^{(2, N_f)}$	71	24	20, [2, 4, 6, 6, 6]	535
$\mathcal{R}_{+++}^{(2, 1)}$	109	49	21, [5, 4, 3, 3, 3]	1092
$\tilde{\mathcal{R}}_{-++}^{(2, N_f)}$	3546	88	47, [4, 4, -5, 3, 4]	24582
$\mathcal{R}_{-++}^{(2, 1)}$	4732	174	48, [1, -3, -6, 2, 2]	29059

- By contrast, in Mandelstams the Ansatz size would be ${}^5C_{32} = 58905$.

How Long Would the Reconstruction Take?

Hypothetical timing breakdown

- Ansatz generation with $29k$ entries ≈ 15 sec. (single core)
- Solving a linear system with $29k$ unknowns ≈ 30 min. (laptop GPU)
- Evaluation of the remainder ≈ 20 min. $\times 29k \approx 1.1$ CPUy.

But do we actually need $29k$ samples?

The most complicated coefficient

$$\tilde{r}_{173}^{(2,1)} = \frac{\mathcal{N}_{173}}{([12]^2[13]^2\langle 14 \rangle^3\langle 15 \rangle^3[23]^2\langle 24 \rangle^2[24]^2\langle 25 \rangle^2[25]^2[34]^2[35]^2\langle 45 \rangle^3 \times \langle 1|2+4|1\rangle\langle 1|2+5|1\rangle\langle 2|1+5|2\rangle\langle 4|1+2|4\rangle^2\langle 4|1+5|4\rangle^2\langle 5|1+2|5\rangle^2\langle 5|1+4|5\rangle^2)}$$

- Without the spurious $\langle k|i+j|k\rangle$ poles we'd need just 2120 samples.

A One-Loop Educated Guess

The $\langle k|i+j|k \rangle$ poles at one loop

- At one loop we can use L_0 to remove one order of $\langle k|i+j|k \rangle$

$$L_0 \left(\frac{-s_{ijk}}{-s_{ij}} \right) \equiv -s_{ij} \ln \left(\frac{-s_{ijk}}{-s_{ij}} \right) \frac{1}{\langle k|i+j|k \rangle}$$

- L_0 does not diverge as $\langle k|i+j|k \rangle \rightarrow 0$, as $\log(1+x) \approx x + \dots$
- $\ln(\mu_R^2 / -s_{ijk})$ comes from the s_{ijk} -bubble, and similarly for s_{ij} .
- Bubble coefficients must be pairwise equal and opposite in these limits.

\implies No denominator should contain two $\langle k|i+j|k \rangle!$

Hypothesize that this also holds at two loops.

Vector Space on Codimension-One Surfaces

Partial fraction decomposition

$$\tilde{r}_{173}^{(2,1)} = \frac{\mathcal{N}_1}{[12]^2[13]^2\langle 14 \rangle^3\langle 15 \rangle^3[23]^2\langle 24 \rangle^2[24]^2\langle 25 \rangle^2[25]^2[34]^2[35]^2\langle 45 \rangle^3\langle 1|2+4|1]} + \frac{\mathcal{N}_2}{[12]^2[13]^2\langle 14 \rangle^3\langle 15 \rangle^3[23]^2\langle 24 \rangle^2[24]^2\langle 25 \rangle^2[25]^2[34]^2[35]^2\langle 45 \rangle^3\langle 1|2+5|1]}$$

... 7 fractions in total ...

- Ansatz size is now $\approx 14k$, down from $29k$. Saved half a CPUy.

Do we actually need all 7 fractions?

- Clearly $\tilde{r}_j \notin \text{span}(\tilde{r}_{i \neq j})$, else it wouldn't be a basis element;
- But as little as 1 fraction may be independent (indeed this is the case!)
- We could predict this with p -adic evaluations on codim.-one surfaces
[see Ben's talk tomorrow]

Algorithm for Simplifying Bases of Vector Spaces

What about all two-particle invariants? Use a vector-space aware Ansatz

- Ideally, define inner product and use Gram–Schmidt (but what's the inner product?)
- Use an Ansatz instead. Replace \tilde{r}_j with \tilde{r}'_j as basis elements

$$\tilde{r}_j = \sum_{i \neq j} a_i \tilde{r}_i + \tilde{r}'_j \text{ with } a_i \in \mathbb{Q}$$

- Sequentially lower pole orders in \tilde{r}'_j as long as the RHS Ansatz fits

What used to be the hardest coefficient

- Actually $\tilde{r}_{173}^{(2,1)}$ is obtained via symmetries now, so I give the next one

$$\tilde{r}_{172}^{(2,1)(\prime)} = \frac{2\langle 13 \rangle [14]^2 \langle 24 \rangle \langle 34 \rangle [45]}{\langle 45 \rangle \langle 4 | 1 + 3 | 4 \rangle^3} + \frac{-2[14] \langle 25 \rangle \langle 34 \rangle^2 [45]}{\langle 45 \rangle^2 \langle 4 | 1 + 3 | 4 \rangle^2} + \frac{-2[14] \langle 24 \rangle \langle 34 \rangle \langle 35 \rangle}{\langle 45 \rangle^3 \langle 4 | 1 + 3 | 4 \rangle}$$

Complexity of the Results

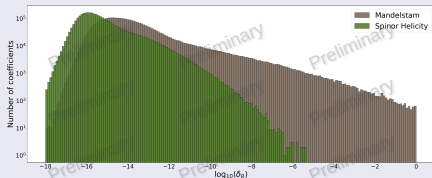
- In parallel, we also performed the calculation w/ the usual Mandelstam ansatz

Contribution	Leaf Count Ratio	Contribution	Leaf Count Ratio
$A_{+++}^{(2,N_f)}$	1.02%	$\tilde{A}_{+++}^{(2,N_f)}$	4.47%
$A_{(2,0)}^{+++}$	2.25%	$A_{(2,1)}^{+++}$	2.96%
$A_{(2,N_f)}^{+++-}$	7.10%	$\tilde{A}_{(2,N_f)}^{+++-}$	6.11%
$A_{(2,0)}^{-++}$	9.05%	$A_{(2,1)}^{-++}$	6.93%

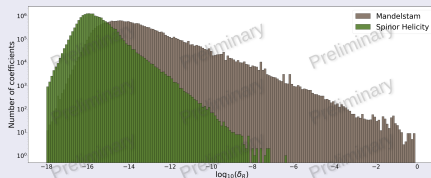
- Mandestam ansatz + partial fraction decomposition
- Spinor ansatz + symmetries + basis simplification + partial fraction
- All spinor remainder bases (planar + non-planar) are $\approx 300\text{kB}$

Numerical Stability of Pentagon Function Coefficients

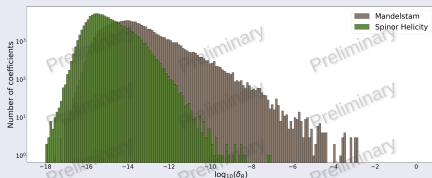
Relative errors of 16-digits vs. 64-digits evaluations (log-log plots)



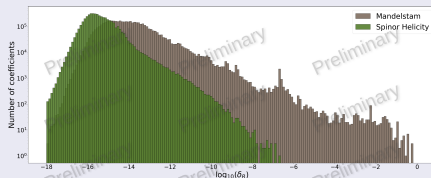
(a) Relative error for \tilde{r}_i in $\tilde{\mathcal{R}}_{+++}^{(2, N_f)}$



(b) Relative error for \tilde{r}_i in $\tilde{\mathcal{R}}_{-++}^{(2, N_f)}$



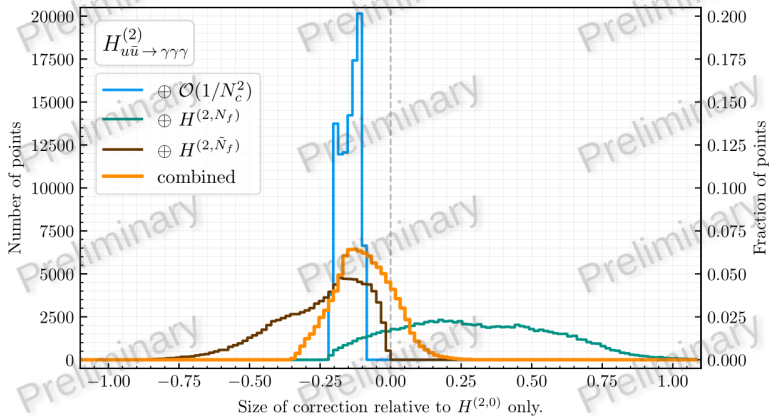
(c) Relative error for \tilde{r}_i in $\mathcal{R}_{+++}^{(2, 1)}$



(d) Relative error for \tilde{r}_i in $\mathcal{R}_{-++}^{(2, 1)}$

Hard Functions - Size of Corrections

Preliminary result: a shift on average of -13%



Thanks for your attention!

Questions?

Backup Slides

Exploiting the Symmetries of the Amplitudes

Number of coefficients we actually need

- Vector spaces of rational functions are closed under symmetries of \mathcal{A}

Contribution	Symmetry (\mathcal{S})	$\dim(\text{span}(r_i))$	\dim “modulo” \mathcal{S}
$\tilde{\mathcal{R}}_{+++}^{(2, N_f)}$	$\mathcal{S}_3[3, 4, 5]$	24	8
$\mathcal{R}_{+++}^{(2, 1)}$	$\mathcal{S}_3[3, 4, 5]$	49	20
$\tilde{\mathcal{R}}_{-++}^{(2, N_f)}$	$\mathcal{S}_2[4, 5]$	88	50
$\mathcal{R}_{-++}^{(2, 1)}$	$\mathcal{S}_2[4, 5]$	174	105

Warning

- these numbers depend on the chosen basis, and can be lowered further!
- but the rational matrix may become denser, and with larger rationals